

Oct 22nd, 12:00 AM

## Ultimate Load Capacity of the Webs of Thin-walled Members

K. C. Rockey

D. M. Porter

H. R. Evans

Follow this and additional works at: <https://scholarsmine.mst.edu/isccss>



Part of the [Structural Engineering Commons](#)

---

### Recommended Citation

Rockey, K. C.; Porter, D. M.; and Evans, H. R., "Ultimate Load Capacity of the Webs of Thin-walled Members" (1973). *International Specialty Conference on Cold-Formed Steel Structures*. 3.  
<https://scholarsmine.mst.edu/isccss/2iccfss/2iccfss-session3/3>

This Article - Conference proceedings is brought to you for free and open access by Scholars' Mine. It has been accepted for inclusion in International Specialty Conference on Cold-Formed Steel Structures by an authorized administrator of Scholars' Mine. This work is protected by U. S. Copyright Law. Unauthorized use including reproduction for redistribution requires the permission of the copyright holder. For more information, please contact [scholarsmine@mst.edu](mailto:scholarsmine@mst.edu).

ULTIMATE LOAD CAPACITY OF THE WEBS OF THIN-WALLED MEMBERS

by

K.C. ROCKEY, D.M. PORTER and H.R. EVANS,  
Department of Civil & Structural Engineering,  
University College, CARDIFF

---

SYNOPSIS

The paper establishes that the new method which the Authors have developed for determining the failure load of conventional plate girders can be used to predict to a very good degree of accuracy the failure load of light gauge symmetrical I-girders.

INTRODUCTION

In a recent investigation carried out by the Authors on behalf of the Merrison Box Girder Committee a number of transversely stiffened plate girders were tested in which the thickness of the flanges was very close to that of the web. This study established that the ultimate load of such plate girders could be predicted using the Rockey-Skaloud collapse mechanism. (1)

However, as a result of a series of tests conducted on longitudinally stiffened plate girders, (2) it became apparent that it was desirable to develop a method for determining the failure load of a plate girder which utilized a failure mechanism involving both the tension and the compression flanges. This has resulted in the authors developing an improved method

for determining the failure load of plate and box girders.<sup>(3)</sup> One pleasing feature of this new method is that in addition to providing a simpler solution procedure it embraces within it as special cases the Basler,<sup>(4)</sup> Wagner,<sup>(5)</sup> Rockey and Skaloud<sup>(1)</sup> and other solutions.<sup>(6,7)</sup>

In view of the authors' success in being able to predict the collapse loads of the plate girders tested for the Merrison Box Girder Committee and also those of earlier investigations,<sup>(3)</sup> it was decided to test eight girders having proportions similar to those which could be encountered in light gauge building construction in order to further confirm the applicability of this new ultimate load method of design to this class of structure.

#### THEORY

In the present paper, no review will be given of the existing methods for determining the ultimate load capacity of plate girders, but a full survey is presented in references (3 and 8).

#### ULTIMATE LOAD CAPACITY OF SHEAR WEBS

##### STAGE 1

If we have a perfectly flat plate then prior to buckling there is a uniform shear stress throughout the panel. Thus there will be a principal tensile stress of magnitude  $\tau$  acting at  $45^\circ$  to the flange and a principal compressive stress of the same magnitude acting at  $135^\circ$ , as shown in Figure 1.

This stress system exists until the shear stress  $\tau$  equals the critical shear stress  $\tau_{cr}$ .

STAGE 2

Once the critical shear stress  $\tau_{cr}$  is reached the panel cannot sustain any increase in compressive stress and buckles. There is then a change in the load carrying system and any additional load has to be supported by a tensile membrane stress  $\sigma_t$ , see Figure 2. Under the action of this membrane stress, the flanges bend inwards and the stress distribution developed in the web is greatly influenced by the rigidity of the flanges.

If the flanges have a very high flexural rigidity, then this membrane stress field  $\sigma_t$  will develop uniformly across the depth of the web plate acting at an angle of approximately  $45^\circ$  to the flanges. However, in the case of girders with weaker flanges which undergo greater inward bowing due to the action of the membrane stress field, both the inclination and the width of the membrane field change, both decreasing with reducing flange stiffness.

STAGE 3

In the case of most practical girders, the membrane stress field at the point of collapse can be approximated by the two stress fields shown in Figure 3. Note that this does not imply that the membrane field acts along the direction of the diagonal - it can adopt an off-diagonal position as shown by Basler.<sup>(4)</sup>

In REGION A it is assumed that only the critical shear stress  $\tau_{cr}$  is acting.

There is ample experimental evidence to show that this

assumption is reasonable. Figure 4 shows a conventional model plate girder tested by Rockey.<sup>(9)</sup> A brittle lacquer was used to record the distribution of the strains developed in the web of the girder and the directions of the principal tensile strains have been marked in chalk. It will be noted that the chalk lines, which indicate areas of high strain, do not extend into the triangular gussets corresponding to the "A" Regions.

The second region is the HIGHLY STRESSED REGION - shown dotted in Figures 2 and 3 in which the critical shear stress  $\tau_{cr}$  acts together with the membrane stress  $\sigma_t$ .

The mid plane tensile membrane stress  $\sigma_t$  increases until it reaches a value of  $\sigma_t^Y$  when acting with the critical shear stress  $\tau_{cr}$  it causes the web to yield. The membrane stress  $\sigma_t$  which produces this yielding is defined as  $\sigma_t^Y$ . Failure occurs, see Figures 5 and 6, when hinges have formed in the flanges which together with yielded portion WXYZ of the web forms a plastic mechanism and overall failure of the girder is thus obtained.

It should be appreciated that plastic yielding could and undoubtedly does extend beyond the boundaries of the region WXYZ, but it is a minimum requirement that the complete Region WXYZ must yield for a mechanism to develop.

#### DETERMINATION OF THE ULTIMATE SHEAR CAPACITY OF THE GIRDER ( $V_{ult}$ )

Consider the equilibrium of the stress field which acts at the ultimate load condition, see Figures 5 and 6. Let the direction of the membrane stress  $\sigma_t^Y$  be inclined at  $\theta$  to the flange.

Now as mentioned previously the inclination of the membrane field will depend on the effective flexural stiffness of the flange members.

Consider the Region WXYZ cut out from the plate and replace the action of the adjacent plates by the boundary stresses, as shown in Figure 6.

Consider a virtual rotation  $\phi$  of the plastic hinges, in an upward direction as shown in Figure 6. Only those stresses acting on the inclined right hand web section YZ and flanges will do the work. Note, however, that in the particular case under consideration, i.e. a symmetrical girder under a predominantly shear loading, the work done by the stresses acting on the flanges will be self cancelling. Therefore

$$\begin{aligned}
 V_{ult} \times c\phi &= 4M_p \phi + \sigma_t^Y t_w (ZP) \sin \theta (c\phi) + \tau_{cr} d_w t_w (c\phi) \\
 V_{ult} &= \frac{4M_p}{c} + \sigma_t^Y t_w d_w \cot \theta - (b_w - c) \sin \theta \sin \theta + \tau_{cr} d_w t_w \\
 &= \frac{4M_p}{c} + c \sigma_t^Y t_w \sin^2 \theta + \sigma_t^Y t_w d_w (\cot \theta - \cot \theta_d) \sin^2 \theta \\
 &\quad + \tau_{cr} d_w t_w \qquad (1)
 \end{aligned}$$

Where  $M_p$  is the full plastic moment of the flange and  $\theta_d$  is the inclination of the panel diagonal.

The internal plastic hinge will occur at the point of max B.M., which occurs where the shear is zero, therefore

$$c(\sigma_t^Y t_w) \sin^2 \theta \frac{c}{2} = 2M_p$$

Hence,  $c = \frac{2}{\sin \theta} \sqrt{\frac{M_p}{\sigma_t^Y t_w}}$  This expression is valid over the range  $0 < c < b$ .

Thus,

$$V_{ult} = 4 \sqrt{M_p \sigma_t^y t_w} \sin \theta + \sigma_t^y t_w d_w (\cot \theta - \cot \theta_d) \sin^2 \theta + \tau_{cr} d_w t_w \quad (2)$$

Where

$$\sigma_t^y = -\frac{3}{2} \tau_{cr} \sin^2 \theta + \sqrt{\sigma_{yw}^2 + \tau_{cr}^2 \left(\frac{3}{2} \sin^2 \theta_d\right)^2 - 3}$$

Since  $V_{ult}$  will vary with the angle of inclination,  $\theta$ , of the stress field it is necessary to find that value of  $\theta$  which will yield the maximum value of  $V_{ult}$ . Since for a given value of  $\theta$ ,  $V_{ult}$  is obtained by direct substitution into equation 2, this is most readily accomplished using a simple computer programme. This procedure is illustrated in Figure 7 which gives the particular solution for girder LG. 6. In reference<sup>(8)</sup> charts are presented which show how the angle  $\theta$  and the ultimate load  $V_{ult}$  varies with the value of the plastic moment  $M_p$  possessed by the flanges.

Although in the solution presented in the present paper is for the case where  $M_p$  is the same for both the tension and compression flanges this is not a restriction and the method can be readily applied to cases where the tension and compression flanges have different effective flexural rigidity.

It is of interest to examine what happens when the flanges have zero  $M_p$ .

In this case the ultimate load is given by:

$$V_{ult} = \sigma_t^y t_w d_w (\cot \theta - \cot \theta_d) \sin^2 \theta + \tau_{cr} d_w t_w$$

This is identical to the true "Basler" solution<sup>(3)</sup> for the case of zero flange stiffness. Thus it is seen that the true Basler Solution is a particular case of the Authors' general

---

solution.

Another practical case of importance is that of a plate girder having a thick web, in this case the web yields before buckling and it cannot develop any tensile membrane field. Consequently there is no lateral loading on the flanges and  $c = b$ . Thus,

$$V_{ult} = \frac{4Mp}{b} + \tau_{yw} t_w d_w$$

This corresponds to a yielded web and a frame mechanism with corner hinges as would be obtained from a normal engineering analysis and is in agreement with the Calladine<sup>(6)</sup> solution for this case. Another limiting case is when the flanges are of such strength that no internal hinges form.

In this case  $c = b$  and the max tensile stress does not slip from the original 45° direction because there is no inward bowing of the flanges.

$$V_{ult} = \frac{4Mp}{b} + \frac{\sigma_t^y t_w d_w}{2} + \tau_{cr} d_w t_w$$

If the web slenderness ratio  $\frac{d_w}{t_w}$  is high then  $\tau_{cr} \rightarrow 0$  and  $\sigma_t^y \rightarrow \sigma_{yw}$  in which case

$$V_{ult} = \frac{4Mp}{b} + \frac{\sigma_{yw} t_w d_w}{2}$$

This agrees both with Wagner's original solution<sup>(5)</sup> for an infinitely long plate having a thin web and rigid flanges and with Calladine's recent treatment.<sup>(6)</sup>

Thus it has been seen that the authors' new solution agrees with all of the limiting classical solutions.

For brevity the foregoing theory is for panels under shear only but in practice shear will always be accompanied by bending.



Thus modified values must be employed for the critical shear stress and  $\sigma_t^Y$ . Also the plastic moment of resistance of the flange must be reduced to allow for the effect of axial stresses produced by the bending moment and the horizontal component of the membrane stress field. Details of these modifications are given in references (3) and (8).

It should be also noted that as in the original Rockey-Skaloud mechanism<sup>(1)</sup> a depth of web of  $30t \left(1 - \frac{2\tau_{cr}}{\tau_{yw}}\right)$  is assumed to act with the flanges.

#### EXPERIMENTAL INVESTIGATION

##### DETAILS OF GIRDERS

In order to demonstrate that the preceding theory is capable of predicting the collapse load of light gauge structures, eight model light gauge beams have been tested to failure. Details of the beams tested are given in Figures 8 and 9, see also Table 1.

The girders were simply supported at their ends as shown in Figures 8, 9 and 10. The central load was applied to the girder by means of a hydraulic jack and measured with a load cell.

Girders LG. 1 - 6 inclusive and LG. 8 were constructed with panels having a nominal panel aspect ratio of 2 to 1, and LG. 7 and 9 with an aspect ratio of 1 to 1.8. The nominal web and flange thicknesses were the same for all girders but the flange widths varied, see Table 1.

All of the girders were fabricated in the Department's workshops using CO<sub>2</sub> welding. In order to assist in the fabri-

ection of the girders the flange-web junction shown in the insets in Figures 8 and 9 was employed.

#### TESTING PROCEDURE

Since the main purpose of the present test series was to ascertain whether or not the theory would adequately predict the failure load of the girders - little instrumentation was employed in the tests on girders LG.1 - 6. In these tests the only measurements that were taken were the vertical displacement of the girder and the inward bowing of the compression and tension flanges. The vertical deflection of the girder was recorded using a dial gauge graduated in units of 0.01 mm. The inward bowing of the flanges were recorded using a transducer travelling on a carriage-way which was placed on the flanges as illustrated in Figure 11. The transducer was connected to an x-y plotter providing a continuous trace of the deformation of the flanges, e.g. see Figure 12 which shows typical traces obtained for girder LG.7. In addition a brittle lacquer was used on several of the girders to record the direction of the principal tensile strains in the web panels and the flanges.

However, a number of strain gauges were attached to the flanges and webs of girders LG.7 and 8.

A standard testing procedure was adopted throughout the tests, the central load was applied in small increments and the vertical deflection recorded and immediately plotted. When the load-deflection curve departed from linearity the loading increments were reduced and all creep allowed to take place before the next load increment was applied. During the period of creep

the deflections were recorded at specific time intervals. Figure 13 shows a typical load-deflection plot.

Tensile test pieces had been cut from the sheet used in the flanges and the webs of the girders and accurate stress-strain curves were obtained, see Figure 14 which gives a typical stress strain curve. The results obtained are given in Table 1.

#### DISCUSSION OF RESULTS

Table 2 gives the test results and their comparison with the predicted ultimate load. It will be noted from this Table that the predicted failure loads are in very close agreement with the experimental failure loads, generally within 2%. However, it is equally important to demonstrate that the proposed model in addition to adequately predicting the failure load does in fact adequately represent the true physical behaviour of the girders. Thus the hinge positions developed in the actual girders together with the predicted hinge positions have been included in Table 2, and it is seen that the proposed collapse mechanism does adequately represent the true physical behaviour of the girders.

One panel of girder LG.6 had been coated with a brittle lacquer which develops cracks at right angles to the principal tensile strain. Figure 15 shows the direction of the tensile field as recorded by this brittle lacquer which is not along the diagonal and which was found to be in close agreement with the predicted inclination of the tension field.

Figure 16 shows the manner in which the stresses developed along the central line of the compression flange. The strain

gauges record the development of an internal plastic hinge in the compression flange at a position close to that obtained from the flange deflection curves.

#### GENERAL DISCUSSION

It will be noted from Figures 17 and 18 which show girders LG.4 and LG.5 after being tested to failure, that when the flange fails, there is some twisting associated with the failure mechanism. It is important, therefore, to check that the flanges will not fail in a torsional mode before the inward collapse occurs. When designing the flanges of light gauge plate girders it is essential to ensure that due allowance be made for the additional flange stresses set up by the tensile membrane field.<sup>(3)</sup> It will be noted from Figure 16 that the strains in the compression flange are significantly greater than would be predicted by simple beam theory. Clearly the present test series have not fully investigated the behaviour of light gauge flanges subjected to a membrane field loading. Further tests are desirable to investigate the behaviour of light gauge flange members when the girder is under the condition of high bending and shear. Now that the present study has shown that the failure loads of light gauge girders subjected to shear can be predicted with a good degree of accuracy, a program of tests to investigate the behaviour of girders under combined shear and bending is in hand.

CONCLUSION

The present experimental study on short light gauge girders subjected to a predominantly shear loading has shown that the ultimate load of such girders can be predicted to a high degree of accuracy by the authors' new method for predicting the collapse behaviour of plate girders.

REFERENCES

1. ROCKEY, K.C., and SKALOUD, M., "The ultimate load behaviour of plate girders loaded in shear," *The Structural Engineer*, Jan. 1972, No.1, Vol. 50, p. 29-47.
  2. ROCKEY, K.C., EVANS, H.R., and PORTER, D.M., "The ultimate load capacity of stiffened webs subjected to shear and bending," Paper No. 4, International Conference on Steel Box Girder Bridges, London, February, 1973.
  3. PORTER, D.M., ROCKEY, K.C., and EVANS, H.R., "An improved and unifying method for determining the ultimate load capacity of plate girders," Departmental Report, University College, Cardiff, February, 1973.
  4. BASLER, K., "Strength of plate girders in shear," *Journal of A.S.C.E.*, October, 1961, ST.7, Proc. No. 2967, Part 1, p. 1951.
  5. WAGNER, H., "Flat sheet metal girders with very thin metal webs," *N.A.C.A.T.M.*, 1931, Nos. 604, 605, and 606.
  6. CALLADINE, C.R., "A plastic theory for collapse of plate girders under combined shearing force and bending moment," *The Structural Engineer*, April, 1973, No. 4, Vol. 51, pp. 147-154.
  7. CHERN, C., and OSTAPENKO, A., "Ultimate strength of plate girders under shear," Fritz Engineering Laboratory Report, August, 1969, Report No. 328.7.
  8. EVANS, H.R., ROCKEY, K.C., and PORTER, D.M., "A method for predicting the ultimate load capacity for plate girders," Departmental Report, University College, Cardiff, June, 1973.
  9. ROCKEY, K.C., "The influence of flange stiffness upon the post-buckled behaviour of web-plate subjected to shear," *Engineering*, 20th December, 1957, p. 788.
-

NOMENCLATURE

$b - b_w$	clear width of web panel
$d - d_w$	clear depth of web panel
$t - t_w$	thickness of web
$t_f$	thickness of flange
$b_f$	width of flange
$b_c$	depth of edge flange lip
$C$	position of plastic hinge in flange
$M_p$	plastic moment of resistance of flange
$V_{ult}$	ultimate panel shear
$V_{PRE}$	predicted panel shear
$W_{exp}$	experimental failure load of girder
$\sigma_t$	membrane tensile stress
$\sigma_t^y$	membrane stress to produce yield
$\sigma_{yw}$	yield stress of web material
$\sigma_{yf}$	yield stress of flange material
$\tau$	shear stress
$\tau_{cr}$	critical shear stress
$\tau_{yw}$	shear yield stress of web material
$\theta$	inclination of membrane stress
$\theta_d$	inclination of panel diagonal
$\phi$	virtual rotation

GIRDER	$b_w$ in	$d_w$ in	$t_w$ in	$b_f$ in	$t_f$ in	$b_c$ in	$\sigma_{yw}$ ton/in <sup>2</sup>	$\sigma_{yf}$ ton/in <sup>2</sup>
LG.1	29.75	14.98	.038	4.00	.038	0.86	11.16	11.16
LG.2	29.67	14.93	.039	4.125	.077	0.86	10.77	13.12
LG.3	29.87	14.95	.036	4.00	.077	0.77	12.90	13.91
LG.4	29.75	14.88	.038	4.125	.077	1.05	11.16	11.36
LG.5	29.82	14.93	.039	5.125	.077	1.10	11.45	11.36
LG.6	29.70	14.83	.039	6.125	.077	1.10	11.45	11.36
LG.7	26.63	14.88	.038	5.125	.077	1.19	13.68	11.56
LG.8	29.81	14.93	.038	6.125	.077	1.13	13.16	11.43
LG.9	26.88	14.87	.038	7.125	.077	1.13	13.42	11.56

TABLE I

DETAILS OF GIRDERS



GIRDER	Comp. flange		Tension flange		Failure load (T)		Predicted inclination of tension field ( $\theta$ )	Remarks
	c/b expt.	c/b predicted	c/b expt.	c/b predicted	Exptl.	$V_{PRE}/V_{exp}$		
LG.1	PILOT	TEST						
LG.2	0.22	0.28	0.35	0.35	3.45	0.99	19°	Presence of flange twisting
LG.3	0.26	0.26	0.33	0.34	3.40	1.00	18°	"
LG.4	0.23	0.28	0.37	0.37	3.50	0.98	19°	"
LG.5	0.18	0.30	0.36	0.38	3.80	0.98	19°	"
LG.6	0.23	0.32	0.35	0.38	3.85	0.98	19°	"
LG.7	0.25	0.29	0.37	0.39	4.20	1.06	20°	No flange twisting
LG.8	0.25	0.30	0.37	0.37	4.05	0.99	18°	"
LG.9	0.33	0.32	0.35	0.38	4.50	0.98	20°	"

TABLE 2  
COMPARISON OF TEST RESULTS WITH PREDICTED VALUES

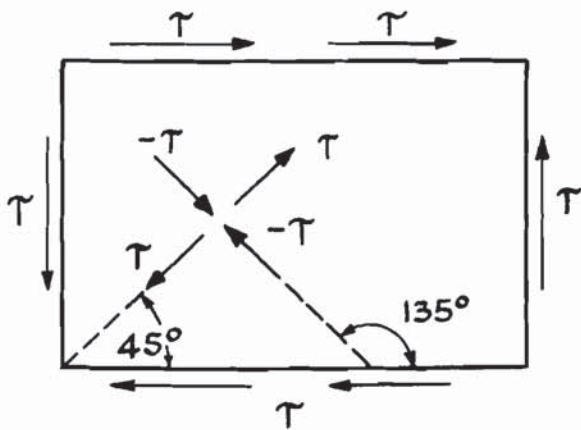


FIG. 1 STAGE 1 - PURE SHEAR  $\tau \leq \tau_{CR}$

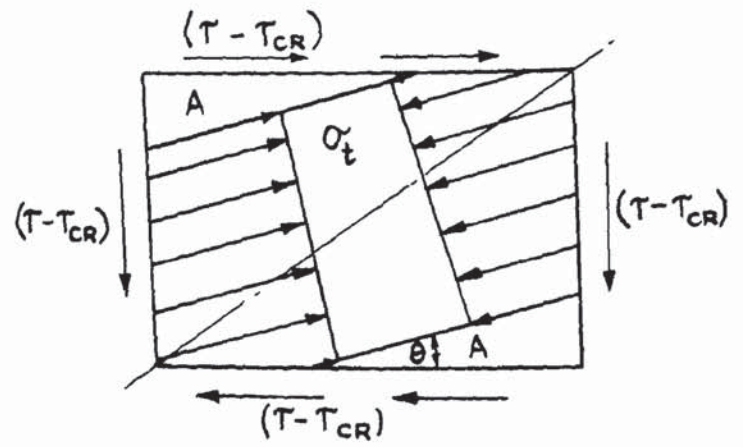


FIG. 2 ADDITIONAL STRESSES SET UP IN POST BUCKLING RANGE.

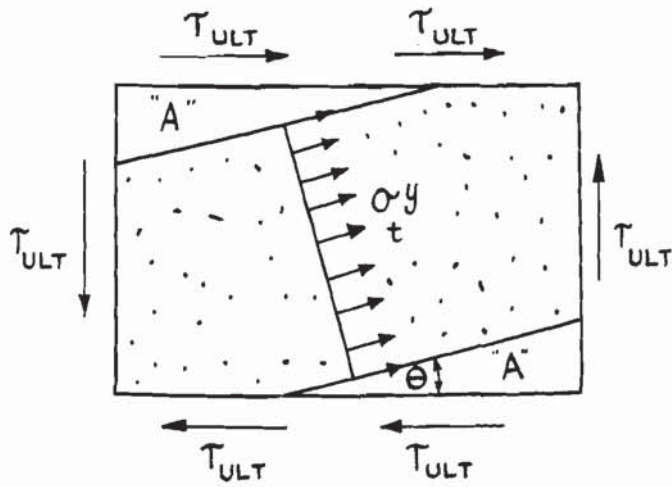


FIG. 3 ASSUMED STRESS DISTRIBUTION  
IN WEB AT COLLAPSE OF  
SHEAR PANEL

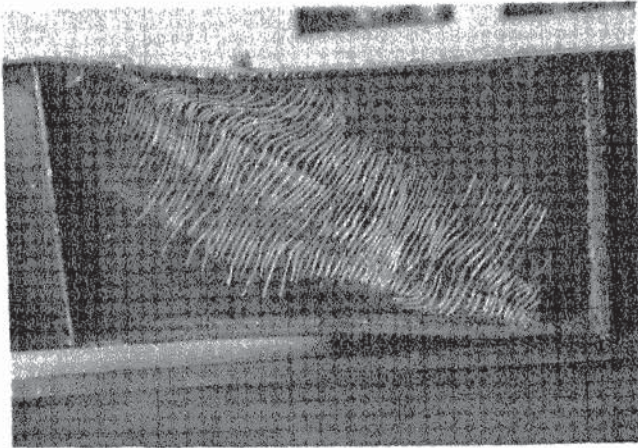


FIG. 4 STRESS DISTRIBUTION AT COLLAPSE OF A  
CONVENTIONAL PLATE GIRDER SHOWING AREA  
OF TENSILE MEMBRANE FIELD

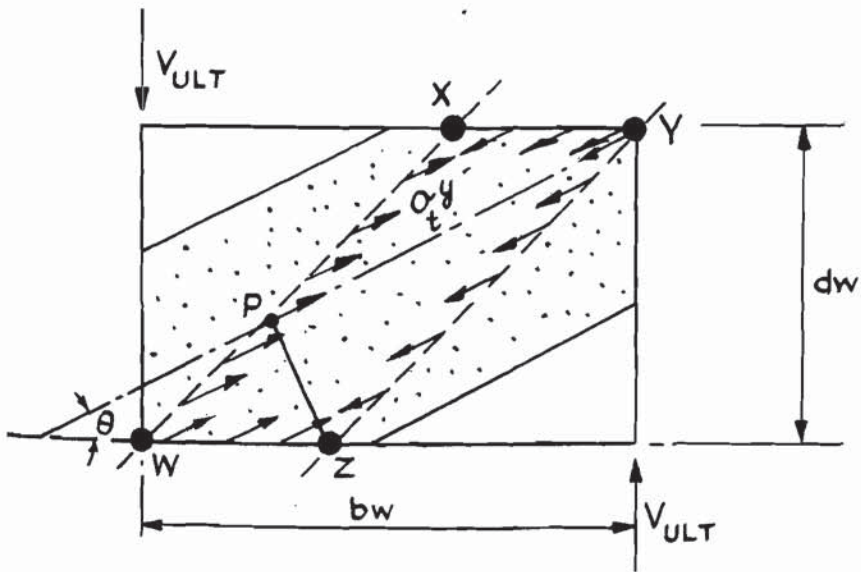


FIG. 5

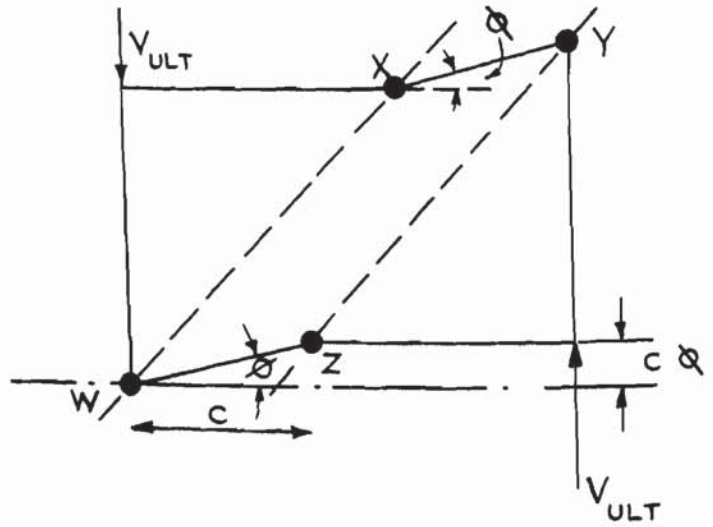


FIG. 6

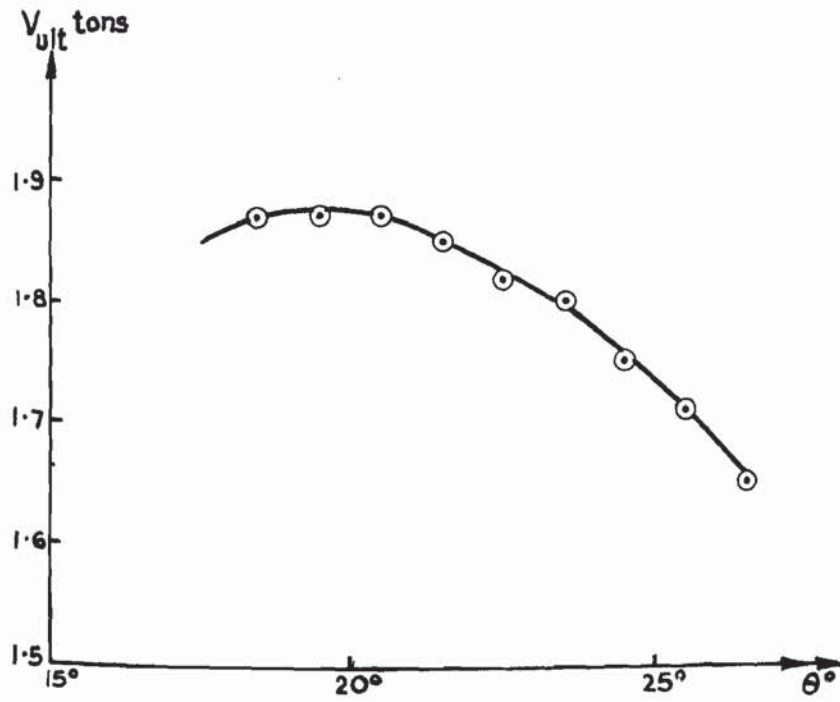
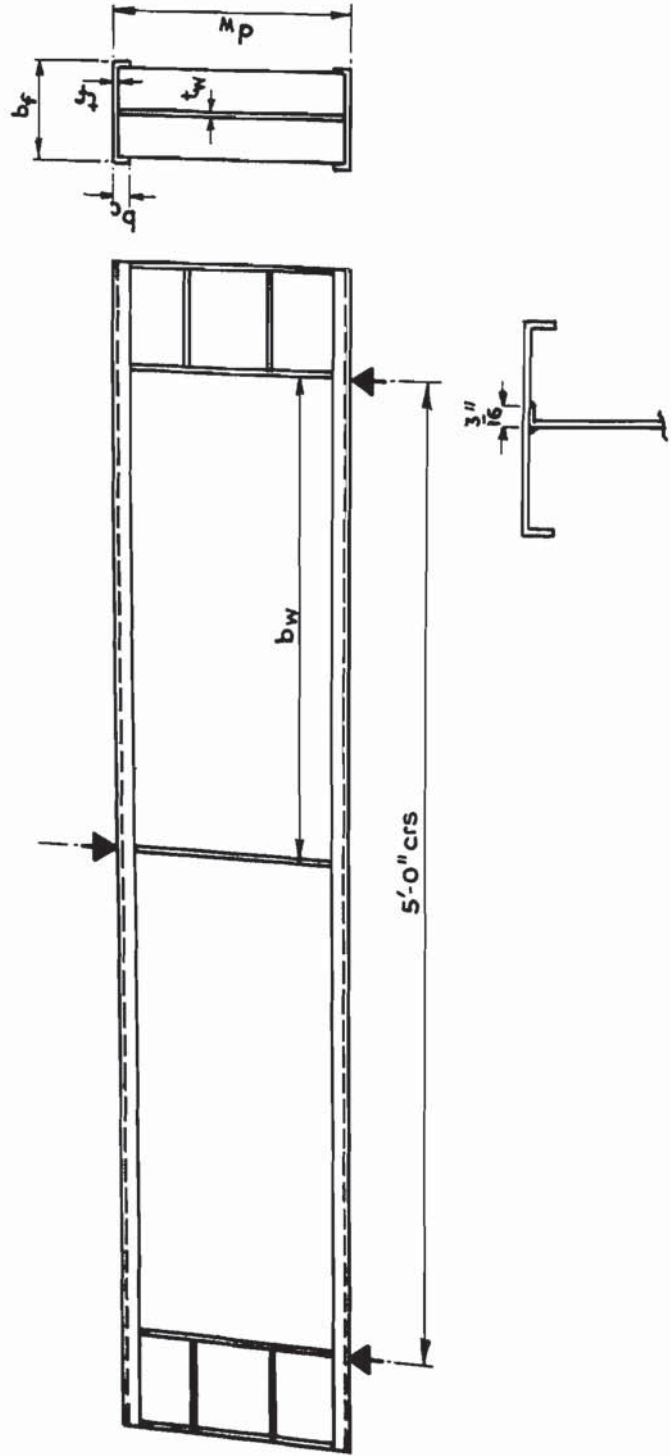


Fig. 7. Variation of Ultimate Load with Inclination of Membrane Field.





Detail of Flange-Web Attachment .

Fig.8 . Girders LG 1-6 incl. and LG 8

LOAD CAPACITY OF WEBS

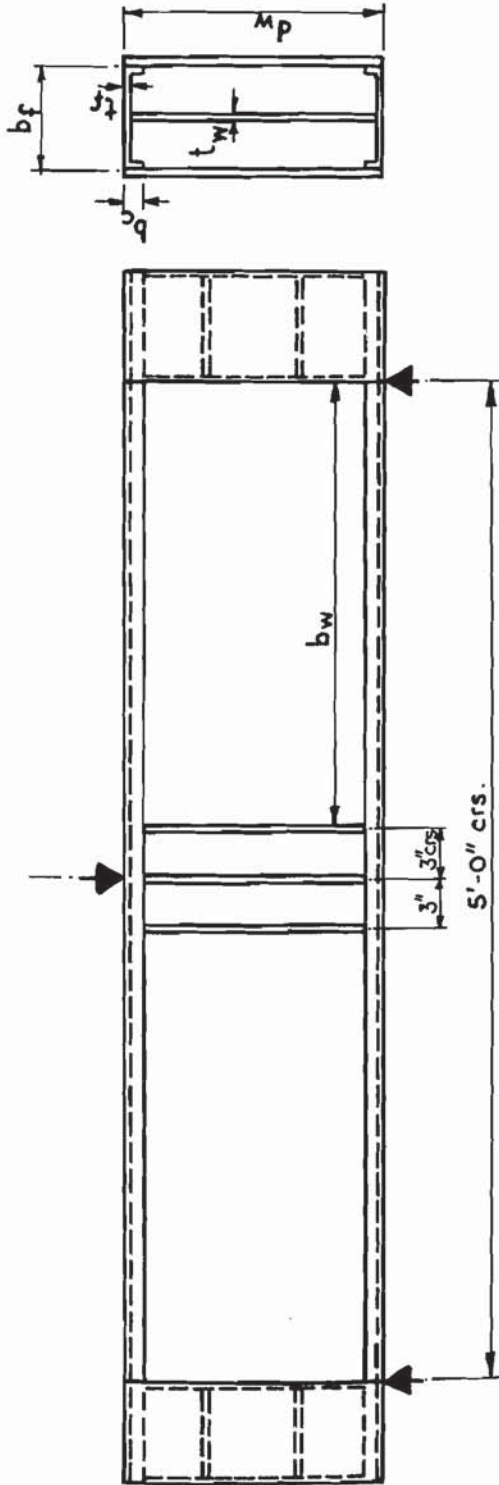


Fig. 9. Girders LG7 and LG9

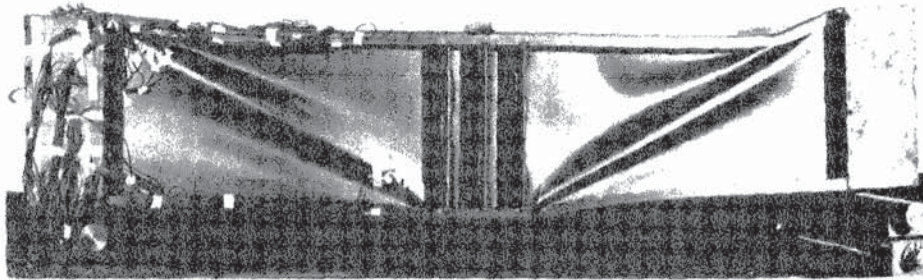


FIG. 10 GIRDER LG9 AFTER FAILURE SHOWING SUPPORT AND LOADING POSITIONS

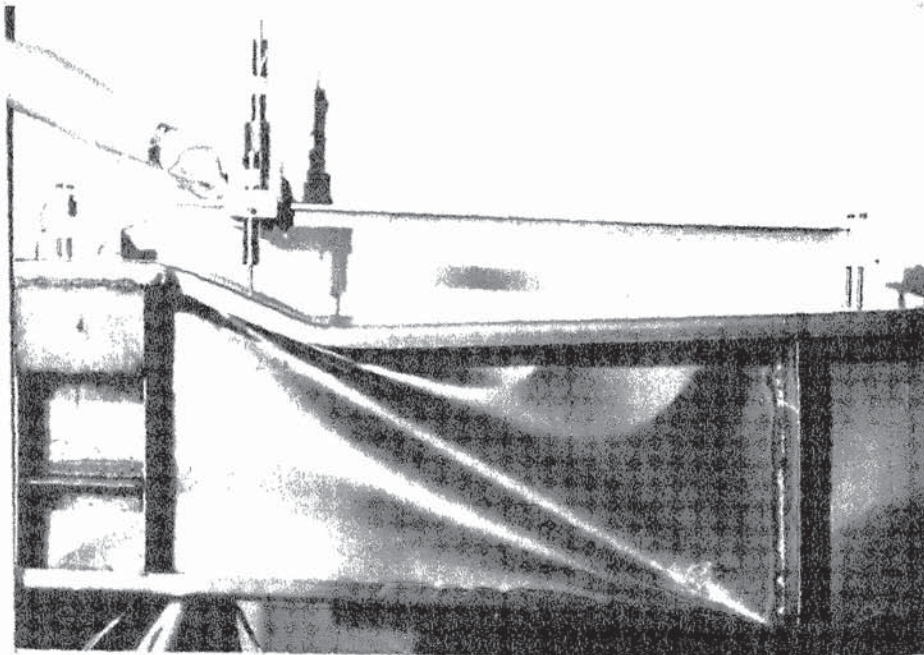


FIG. 11 TRANSDUCER AND CARRIAGE-WAY TO DETERMINE DEFLECTION PROFILE

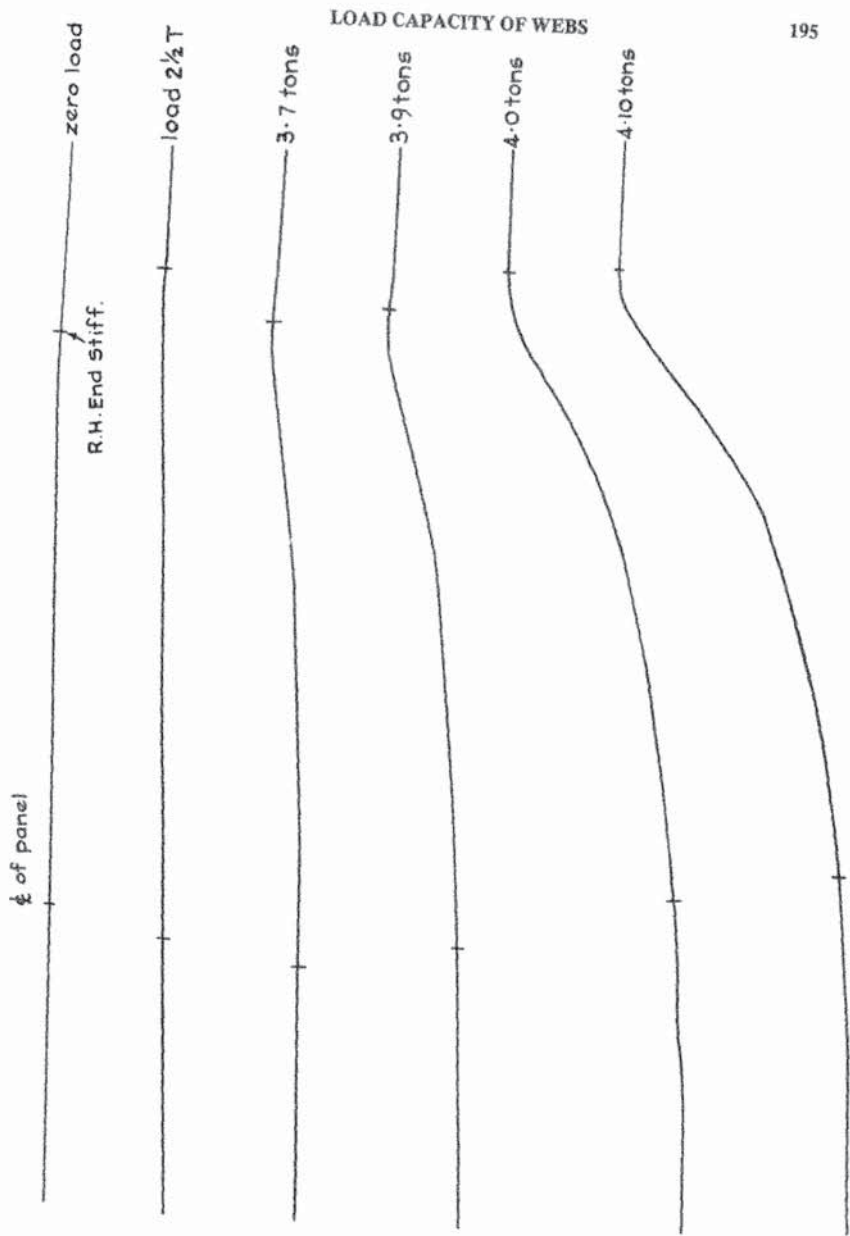


Fig. 12. Deflection Trace of Compression Flange. R. H. Panel Girder L G 7.

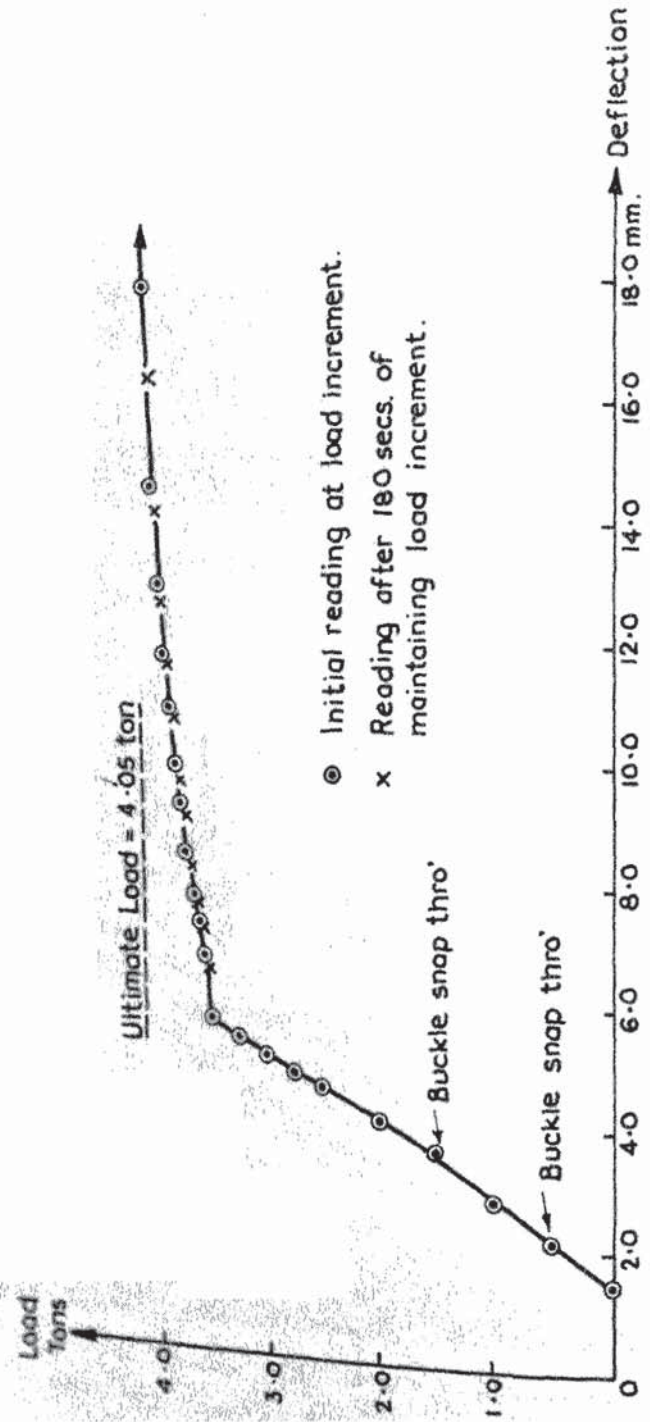


Fig.13. Load/Central Deflection for LG8.

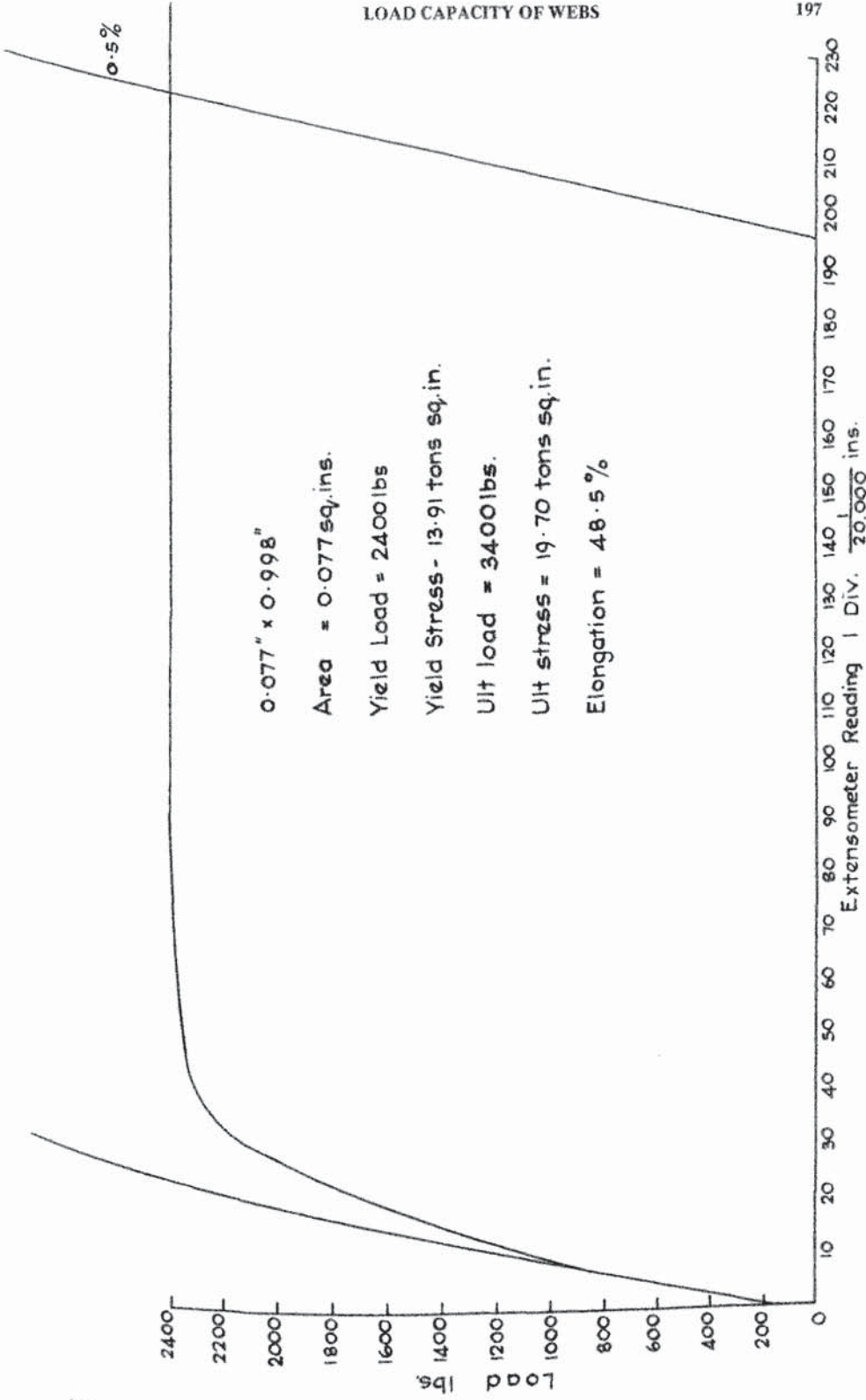


FIG. 14. LOAD / EXTENSION PLOT FLANGE MATERIAL GIRDER LG3.

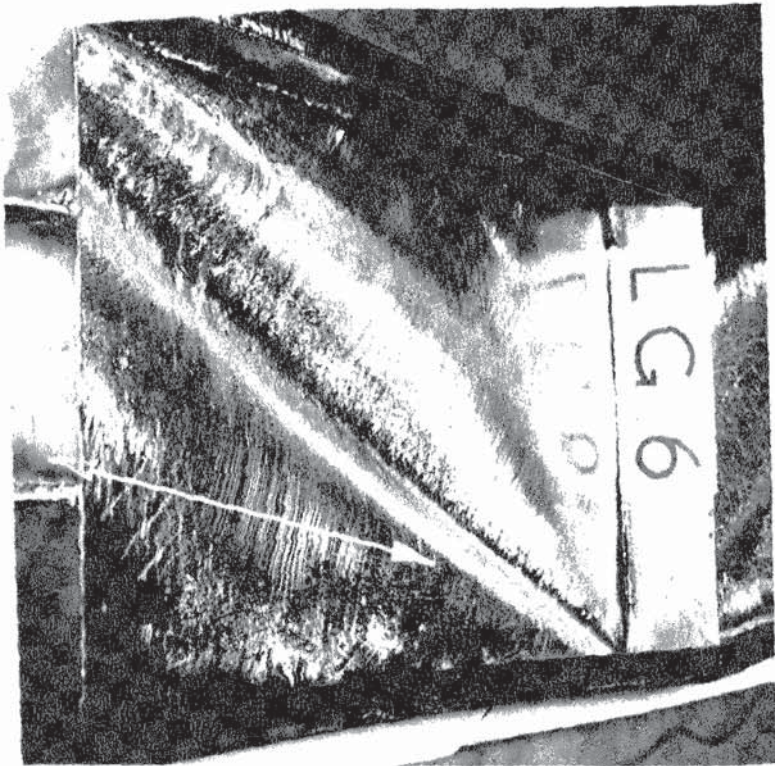


FIG. 15 GIRDER LG6 AFTER TEST TO FAILURE. CRACKS IN BRITTLE LACQUER INDICATE DIRECTION OF PRINCIPAL TENSILE STRAINS

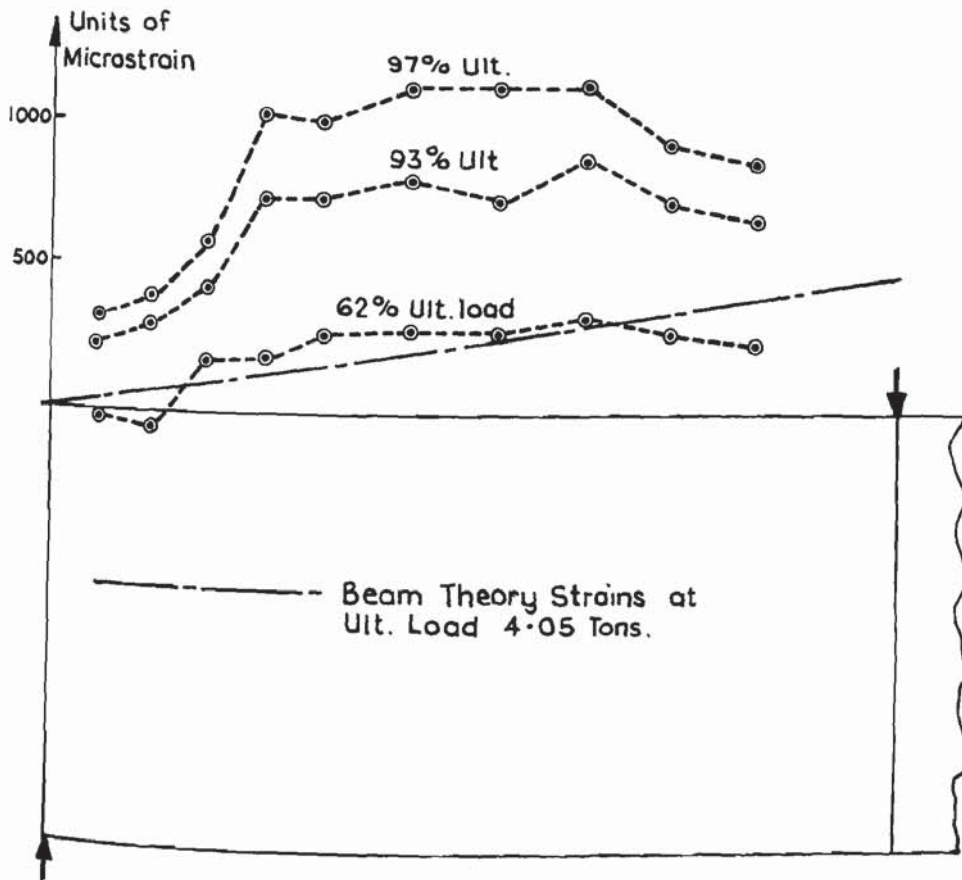


Fig.16. Distribution of Top Surface Strains on Centre Line of Compression Flange LG8.



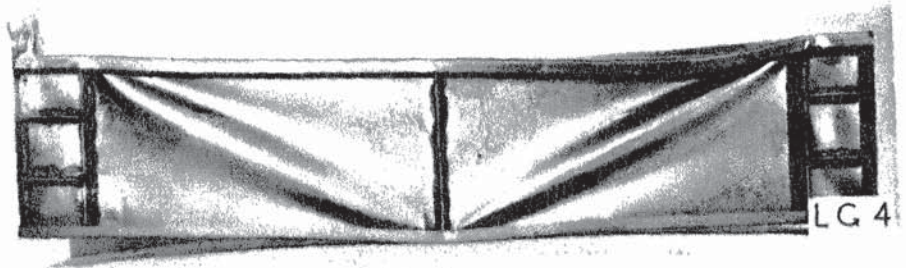


FIG. 17 GIRDER LG4 AFTER FAILURE



FIG. 18 GIRDER LG5 AFTER FAILURE